https://doi.org/10.30799/jnst.157.18040507 J. Nanosci. Tech. - Volume 4 Issue 5 (2018) 487–491

Share Your Innovations through JACS Directory

Journal of Nanoscience and Technology

Visit Journal at http://www.jacsdirectory.com/jnst

ISSN: 2455-0191

Structural, Dielectric and Magnetic Properties of Al^{3+} and Cr^{3+} Substituted Ni-Zn-Cu Ferrites

G. Satyanarayana[1,2], G. Nageswara Rao[2,*], K. Vijaya Babu[1]

[1]*Advanced Analytical Laboratory, Andhra University, Visakhapatnam – 530 003, Andhra Pradesh, India.*
[2]*School of Chemistry, AU College of Science & Technology, Andhra University, Visakhapatnam – 530 003, Andhra Pradesh, India.*

ARTICLE DETAILS

Article history:
Received 21 August 2018
Accepted 29 August 2018
Available online 31 August 2018

Keywords:
Ni-Zn-Cu Ferrite
Microstructure
Dielectric Constant
Magnetization

ABSTRACT

Ferrite materials with the general formula $Ni_{0.7}Zn_{0.2}Cu_{0.1}Fe_{1.9}M_{0.1}O_4$ (M=Al and Cr) are synthesized by using the solid state reaction method. X-ray diffraction (XRD), Fourier transforms infrared (FTIR) spectra, scanning electron microscope (SEM) dielectric measurements and vibrating sample magnetometer (VSM) techniques are utilized to study the various properties of the synthesized ferrites. XRD analysis confirmed the formation of single phase cubic spinel structure and the crystallite size is calculated by Scherrer's formula found to be 20.3 and 12.5 nm. The magnetic properties were studied using pulse field hysteresis loop technique at room temperature. The saturation magnetization exhibit 98.71 and 91.69 emu/g for Al^{3+} and Cr^{3+} substituted Ni-Zn-Cu ferrites respectively. The magnetic permeability is increasing for chromium substituted compound in the frequency range 100 Hz to 120 MHz and significant modification in DC conductivity is explained on the basis of hopping mechanism.

1. Introduction

Ferrites are the materials of great importance in technological applications on account of their combined electrical and magnetic properties. They possess very high electrical resistivity, high saturation magnetization, high permeability, low dielectric loss and other properties which makes them usable in different applications [1-3]. Nickel ferrite ($NiFe_2O_4$) is one of the most important spinel ferrite which finds applications in the manufacture of soft magnets and low materials at high frequencies. $NiFe_2O_4$ has an inverse spinel structure. In this structure Ni^{2+} ions occupy octahedron B-sites and Fe^{3+} ions occupy both the tetrahedron A and the octahedron B sites. In spinel structure there are 56 ions, 32 oxygen ions and 24 metal ions in a unit cell. The spinel crystal structure is determined primarily by the oxygen ions lattice. The substitution of different cations in the lattice of the ferrite depends on ionic radii of the constituent ions [4-6]. The chemical composition method of synthesis, nature of dopant, site preference of dopants etc. parameters strongly influences the structural, electrical and magnetic properties of spinel ferrites. Nickel and substituted nickel ferrites are important magnetic materials due to their remarkable properties and therefore they have been widely studied [7-9]. Nickel-zinc ferrites are adequate for use in the high frequency band because of its high resistivity with sufficient low losses for microwave applications and are widely used in electronic devices because of its environmental stability and high performance in the radio frequency region. The effect of substitution of Fe^{3+} by Cr^{3+} in nickel ferrite have been studied by various researchers and showed that Cr^{3+} always seeks to the octahedral sites [10, 11]. Also Al^{3+}substituted Ni-Zn ferrite has been prepared by standard double sintering method and the structural, electrical, dielectric and magnetic properties have been studied [12-14]. In this paper, we present the structural, dielectric and magnetic properties of Al^{3+} and Cr^{3+} substituted Ni-Zn-Cu ferrite system. The compounds are synthesised by solid state reaction method with the general formula $Ni_{0.7}Zn_{0.2}Cu_{0.1}Fe_{1.9}M_{0.1}O_4$ (M=Al and Cr).

2. Experimental Methods

The $Ni_{0.7}Zn_{0.2}Cu_{0.1}Fe_{1.9}M_{0.1}O_4$ (M=Al and Cr) ferrites are synthesized by using solid state reaction method. AR chemicals such as nickel oxide (NiO), zinc oxide (ZnO), copper oxide CuO, iron oxide (Fe_2O_3) and aluminium oxide (Al_2O_3), chromium oxide (Cr_2O_3) are used for the synthesis process. Stoichiometric proportions of these starting materials are accurately weigh and mixed thoroughly. Then first pre-sintering of powder was carried out at 1100 °C for 5 hr. The The powder samples added with polyvinyl alcohol (PVA) as a binder are ground and then pressed at 5 tons/5 minutes pressure into a circular disk shaped pellet. The synthesized powder and pellet is sintered at 1200 °C for 5 hours and then used for further investigations of structural, morphological, magnetic and electrical properties. The surface layers of the sintered pellet are carefully polished and washed in acetone and then the pellet is coated with silver paste on the opposite faces which act as electrodes.

The synthesized $Ni_{0.7}Zn_{0.2}Cu_{0.1}Fe_{1.9}M_{0.1}O_4$ (M=Al and Cr) ferrites are characterized by standard techniques such as X-ray powder diffraction (XRD), scanning electron microscope (SEM), electron spin resonance (ESR) and LCR meter. The XRD patterns are recorded at room temperature in the 2θ range of 10° to 70° using Cu-Kα radiation (λ=1.5405 Å). The particle morphology of the powders is observed using scanning electron microscopy images taken from JEOL JSM-6610L. Fourier transform infrared (FT-IR) spectra measurements are accomplished by Shimadzu IR-Prestige21 instrument in transmittance method with potassium bromide (KBr) as IR window in the wave number region of 400 to 1300 cm^{-1}. The magnetic properties are measured using JEOL-JES-FA100 electron spin resonance (ESR) spectrometer with X-band at room temperature. The impedance study is performed by Wayne-Kerr high frequency LCR meter Model 65120 in the frequency range 100 Hz to 120 MHz at room temperature. Initial permeability is determined by 10 turns of SWG enameled copper wire on toroid's and inductance measurement is carried out at various frequencies using Wayne-Kerr high frequency LCR meter Model 65120 in the frequency range 100 Hz to 120 MHz at room temperature. Magnetic measurements are performed using a Lakeshore 7400 vibrating sample magnetometer up to 15000 Oe at room temperature.

*Corresponding Author:gollapallinr@yahoo.com(G. Nageswara Rao)

https://doi.org/10.30799/jnst.157.18040507
2455-0191 / JACS Directory©2018. All Rights Reserved

Cite this Article as: G. Satyanarayana, G. Nageswara Rao, K. Vijaya Babu, Structural, dielectric and magnetic properties of Al^{3+} and Cr^{3+} substituted Ni-Zn-Cu ferrites, J. Nanosci. Tech. 4(5) (2018) 487–491.

3. Results and Discussion

3.1 Structural Analysis

The X-ray diffraction patterns of the $Ni_{0.7}Zn_{0.2}Cu_{0.1}Fe_{1.9}M_{0.1}O_4$ (M=Al and Cr) ferrites are shown in Fig. 1. The XRD patterns of both the samples show the reflections belonging to cubic spinel structure and no extra peaks have been observed in the XRD patterns. All the reflections seen in the XRD patterns are sharp clear and intense. The single phase formations of compounds under investigations are confirmed from the analysis of XRD pattern. The presence of the strong diffraction peaks corresponding to the planes (111), (220), (311), (222), (400), (422), (511) and (440) indexed using Bragg's law indicates that the presence of cubic spinel ferrite. The strongest reflection comes from the (311) plane, which denotes the spinel phase. Using the XRD data inter-planar spacing d-values are calculated and are listed in Table 1 along with their respective (hkl) planes. As per d-spacing of the nickel ferrite, it is very much clear that it belongs to cubic spinel and there is no deviation from ideal d-spacing values. From the table, it is observed that the minimum d-values are observed for aluminium substituted compound. Fig. 2 clearly shows the shift in 2θ for aluminium substituted ferrite system and the angle shifts towards lower values. This shift is attributed to decrease in lattice parameter. The lattice parameter is calculated using the standard formula $a = d\sqrt{h^2+k^2+l^2}$, here d is inter-planer spacing and (hkl) are Miller indices. The results obtained from unit cell software and above relation are same are given in Table 2. It is clear from the table, that the lattice constant of aluminium substituted compound is smaller than the chromium substituted compound. The lattice constant depends upon the ionic radii of the dopant ions. The difference in lattice constant is due to difference in ionic radii of the aluminium and chromium [15-17]. The variation may be due to difference in the ionic radii of Cr^{3+} (0.62ppm) and Al^{3+} (0.53 ppm) ions. The change of lattice parameters also indicates the change of cation distribution. Table 2 also indicates the values of unit cell volume (V) and molecular weight. The crystalline size is calculated for both the compounds using the high intensity (311) peak and using the Scherrer's formula. It is seen that the crystallite size of the aluminium and chromium substituted nickel ferrites are 9.2875 and 4.9408 nm respectively.

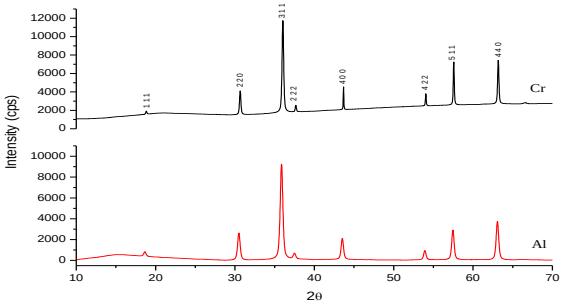

Fig. 1 X-ray diffraction patterns of $Ni_{0.7}Zn_{0.2}Cu_{0.1}Fe_{1.9}M_{0.1}O_4$ (M=Al and Cr)

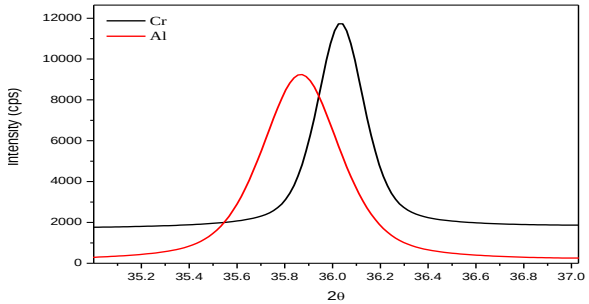

Fig. 2 Enlarged view of (311) peak for $Ni_{0.7}Zn_{0.2}Cu_{0.1}Fe_{1.9}M_{0.1}O_4$ (M=Al and Cr)

Table 1 Inter-planar spacing (d) of $Ni_{0.7}Zn_{0.2}Cu_{0.1}Fe_{1.9}M_{0.1}O_4$ (M=Al and Cr) ferrites

Plane *h k l*	Inter planar distance (Å)	
	Al	*Cr*
1 1 1	4.71525	4.7203
2 2 0	2.91527	2.9500
3 1 1	2.49177	2.5343
2 2 2	2.38783	2.4973
4 0 0	2.07091	2.0889
4 2 2	1.69464	1.6863
5 1 1	1.59869	1.6131
4 4 0	1.46968	1.4720

Table 2 crystallite parameters of $Ni_{0.7}Zn_{0.2}Cu_{0.1}Fe_{1.9}M_{0.1}O_4$ (M=Al and Cr) ferrites

Sample	Lattice constant (nm)	Volume (Å)^3	X-ray density (g.cm^{-3})	Crystallite size (nm)
Al	0.8295	570.9251	5.3700	9.2875
Cr	0.8355	583.3801	5.3337	4.9408

Table 3 Physical properties of $Ni_{0.7}Zn_{0.2}Cu_{0.1}Fe_{1.9}M_{0.1}O_4$ (M=Al and Cr) ferrites

Sample	Saturation magnetization (M_s) (emu/gm)	Magnetic moment (η_B)	Coercivity (H_c) (Oe)	H_r	g-value
Al	98.2837	4.149	21	408.075	1.6548
Cr	90.6144	3.821	31	386.071	1.7496

3.2 FTIR Measurements

Fig. 3 shows the FTIR spectra of $Ni_{0.7}Zn_{0.2}Cu_{0.1}Fe_{1.9}M_{0.1}O_4$ (M=Al and Cr) ferrites. Both the samples consist of two prominent frequency bands around 400 and 600 cm^{-1} indicating both samples have single phase cubic spinel structure. In ferrites, the metal cations are situated in two different sub-lattices which have tetrahedral and octahedral sites. The absorption band ν_1 corresponds to the starching vibration mode of Fe^{3+}-O^{2-} in tetrahedral A-site and ν_2 corresponds to metal-oxygen vibrations in octahedral sites. The difference in the band position is expected because of the difference in the Fe^{3+}-O^{2-} for the octahedral and tetrahedral complexes. From the figure, it can be understand that the ν_1 and ν_2 shifted slightly in aluminium substituted compound. The difference in band positions is attributed to Fe^{3+}-O^2. The higher frequency absorption band ν_1 is assigned to vibrations of the tetrahedral metal complexes which is the bond between the oxygen ion and tetrahedral site metal ion. Lower frequency band ν_2 is assigned to vibration of octahedral metal complexes which is the bond between oxygen ion and octahedral site metal ion [18, 19].

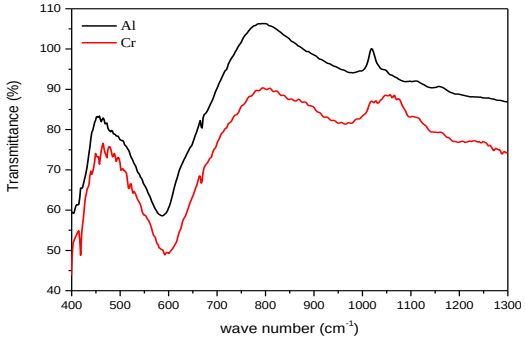

Fig. 3 FTIR spectra of $Ni_{0.7}Zn_{0.2}Cu_{0.1}Fe_{1.9}M_{0.1}O_4$ (M=Al and Cr)

3.3 Morphological Studies

The morphological studies are performed using scanning electron microscope (SEM). Fig. 4(a) and (b) shows the SEM images of $Ni_{0.7}Zn_{0.2}Cu_{0.1}Fe_{1.9}M_{0.1}O_4$ (M=Al and Cr) ferrites. The morphology of the particles is very similar for both the compounds. They indicate that the particle that the particle size of the compounds lies in the nano-meter range having a spherical shape and a narrow size distribution. In both compounds, one can see that the grains are well separated. Also, intra-granular pores are not present on the surface of the grains. Average grain size for both the Al^{3+} and Cr^{3+} compounds are 1.63 and 1.57 μm respectively and it may be the attributed to the higher atomic mobility of ions. The average crystallite size calculated from XRD measurements are found to be consistent with grain size measured from SEM [20].

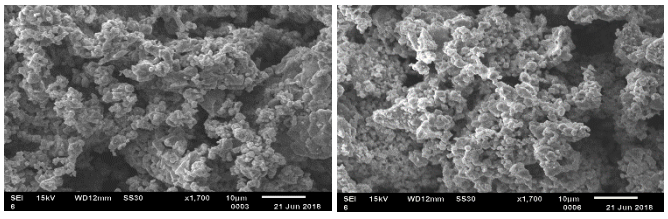

Fig. 4 SEM images of a) $Ni_{0.7}Zn_{0.2}Cu_{0.1}Fe_{1.9}Al_{0.1}O_4$ and b) $Ni_{0.7}Zn_{0.2}Cu_{0.1}Fe_{1.9}Cr_{0.1}O_4$

3.4 Dielectric Constant (ε_r)

The variation of dielectric constant at room temperature in the frequency range from 100Hz to 120MHz for $Ni_{0.7}Zn_{0.2}Cu_{0.1}Fe_{1.9}M_{0.1}O_4$ (M=Al and Cr) ferrites are shown in Fig. 5. It is observed that the dielectric constant decreases with increasing frequency for both the compounds. It may be explained that the dielectric constant in ferrites is attributed to

https://doi.org/10.30799/jnst.157.18040507

four types of polarizations interfacial, dipolar, atomic and electronic. Al low frequencies dipolar and interfacial polarizations are known to play the most important role. The decrease in the value of dielectric constant with increasing frequency upto 100 MHz and it is increasing at higher frequency. The decrease in the dielectric constant with increased frequency suggests that the effect of frequency is more pronounced on the interfacial than on the dipolar polarization. At high frequencies electronic and ionic polarizations are the main contributors and their role is insignificant. Therefore, a low value of the dielectric constant at high frequencies is observed [21, 22].

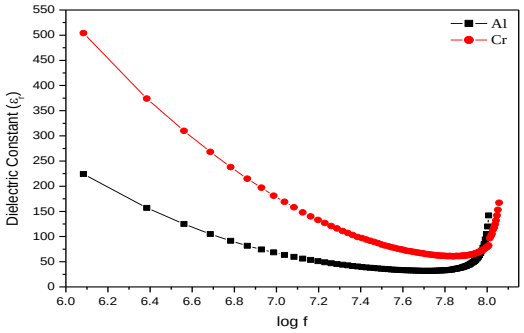

Fig. 5 Variation of dielectric constant with frequency of $Ni_{0.7}Zn_{0.2}Cu_{0.1}Fe_{1.9}M_{0.1}O_4$ (M=Al and Cr)

3.5 Dielectric Loss Tangent (tan δ)

Fig. 6 is a typical curve of the $Ni_{0.7}Zn_{0.2}Cu_{0.1}Fe_{1.9}M_{0.1}O_4$ (M=Al and Cr) ferrites for variation of dielectric loss tangent (tan δ) at room temperature with the frequency range from 100 Hz to 120 MHz. The curve shows that the increases in the tanδ with frequency for both the compounds. This can be attributed to the decrease in the resistivity which causes increase in tan δ. At low frequency, tanδ is low and increases rapidly at high frequency. This can be explain that ferrites system consist of well conducting grain boundaries while thin insulated grain boundaries are more effective at low frequency, however well conducting grain boundaries are more effective at the high frequency region. Hence, it is expected that dielectric loss tangent is less at the low frequency region while it is at because fewer energy is required for the hopping process of the charge carriers, where as it is higher in the high frequency region because extra energy is required for the hopping process of the charge carriers in this region [23, 24].

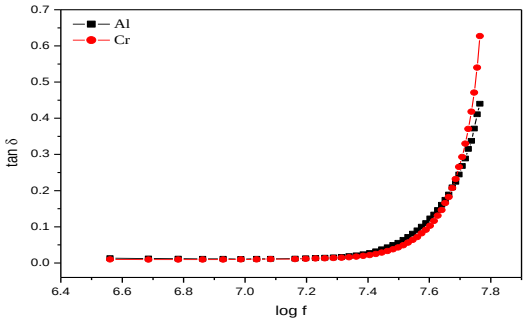

Fig. 6 Variation of dielectric loss of tangent with frequency of $Ni_{0.7}Zn_{0.2}Cu_{0.1}Fe_{1.9}M_{0.1}O_4$ (M=Al and Cr)

3.6 DC Electrical Resistivity

The dc resistivity of the $Ni_{0.7}Zn_{0.2}Cu_{0.1}Fe_{1.9}M_{0.1}O_4$ (M=Al and Cr) ferrites is calculated at room temperature and measuring the value of resistance R. The values of resistivity is calculated by using the following relation,

$$\rho = \frac{RA}{l}$$

where, R is Resistance measured, A is cross-sectional area of the pellet and *l* is thickness of the pellet. Fig. 7 shows the variation of resistivity as a function of frequency. In the present study, Fe^{3+} ions are replaced by Al^{3+} and Cr^{3+} ions. The maximum resistivity is observed for Cr^{3+} substituted ferrite and minimum for Al^{3+} substituted ferrite compound. The substitution ions have strong preference to octahedral B-site which leads to Fe^{3+} ions at B-site. These ions (Al^{3+} and Cr^{3+}) do not participate in the conduction process but it limits the degree of $Fe^{2+} \leftrightarrow Fe^{3+}$ conduction by blocking of Fe^{2+} to Fe^{3+} ions. This results in increase in resistivity with Cr^{3+} substituted compound than Al^{3+} substituted compound. The concentration of Fe^{3+} ions on octahedral B-site decreases with substitution of Al^{3+} and Cr^{3+} ions. The hopping rate of electron transfer will decrease the decrease of Fe^{3+} ions. As a result, the dc resistivity decreases with Al^{3+} ions [25, 26].

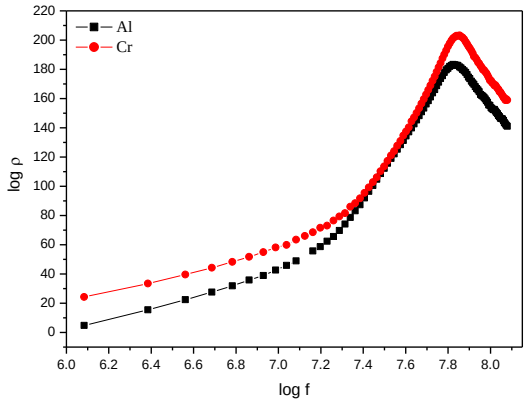

Fig. 7 Variation of log ρ with frequency of $Ni_{0.7}Zn_{0.2}Cu_{0.1}Fe_{1.9}M_{0.1}O_4$ (M=Al and Cr)

3.7 Initial Permeability

The initial permeability of $Ni_{0.7}Zn_{0.2}Cu_{0.1}Fe_{1.9}M_{0.1}O_4$ (M=Al and Cr) ferrites is mainly caused by spin rotation and domain wall displacement at microwave frequencies. The variation of initial permeability with frequency has been carried out using Waynn-Kerr network analyser at room temperature at 20Hz to 120MHz. The initial permeability of toroids is calculated by using the formula

$$\mu_i = \frac{L}{0.0046 N^2 h \log \frac{d_2}{d_1}}$$

where L is the inductance in μH, N is the number of turns, d_1 is the inner diameter in cm, d_2 is the outer diameter in cm and h is the height of the core in cm. From the Fig. 8, the initial permeability increases slowly with frequency and exhibits a small peak near 100 MHz. The sharp fall suggest the single phase formation of ferrite material. The constant values of μ_i over a large frequency range show the compositional stability and quality of the ferrites. Further, the rapid increase in μ_i at higher frequencies is indicative of the onset of resonance. As the resonance frequency represents the high frequency limit up to which the material can be used in device and in this work the resonance is occurring at higher frequencies in both the compounds. This result is also in accordance with Snoek's law. From this law, the initial permeability and saturation magnetization are interdependent. Also this law indicates that, the resonant frequency is low, initial permeability will be high. The value of μ_i is depends significantly on the saturation magnetization, grain size and magnetocrystalline anisotropy. The relationship between grain size and permeability is linear only if the grain growth is normal i.e., if all grains grow at the same time and at the same rate [27, 28].

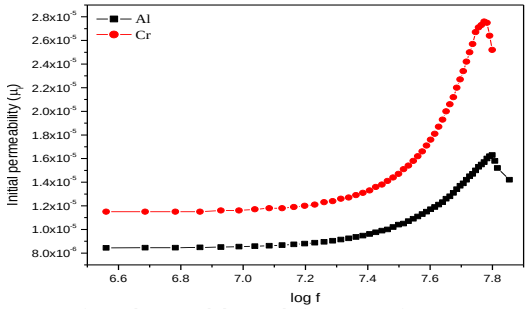

Fig. 8 Variation of initial permeability with frequency of $Ni_{0.7}Zn_{0.2}Cu_{0.1}Fe_{1.9}M_{0.1}O_4$ (M=Al and Cr)

3.8 ESR Studies

The super-exchange interactions and magnetic anisotropy are the magnetic parameters which we can realize through the microscopic magnetic behavior of ferrite system. Electron spin resonance is a promising spectroscopic technique to investigate the magnetic nature of synthesized ferrite materials at the microscopic level. The ESR spectra for the $Ni_{0.7}Zn_{0.2}Cu_{0.1}Fe_{1.9}M_{0.1}O_4$ (M=Al and Cr) ferrites are shown in Fig. 9 and the spectra recorded at a constant microwave frequency in the presence of a magnetic field of 650 mT. It is observed that the ESR spectra consist of two resonance peaks. The resonance signal is shifted towards the lower side of the spectrum for both the compounds. This may be due to the magnetic dipole interactions i.e., super exchange interactions between magnetic ions through oxygen ions is the predominant factor which determine the ESR parameters like g-value and peak to peak resonance line width ΔH_{pp}. the value of Lande's g-factor and spin-spin relaxation time are determined by,

https://doi.org/10.30799/jnst.157.18040507

$$g = \frac{h\upsilon}{\mu_B H_r}$$

where ν is the frequency of electromagnetic radiation, h is Planck's constant, μ_B is Bohr magneton and H_r is the resonance field. The calculated values of resonance field, Lande's g-factor are listed in Table 3. The resonance field decreases whereas g-value increases in Cr^{3+} substituted ferrite system this is due to the isotropic alignment of magnetic moments with substituted ions. The g-value gives information regarding the molecular motion, the paramagnetic properties and the symmetry of ions [29, 30].

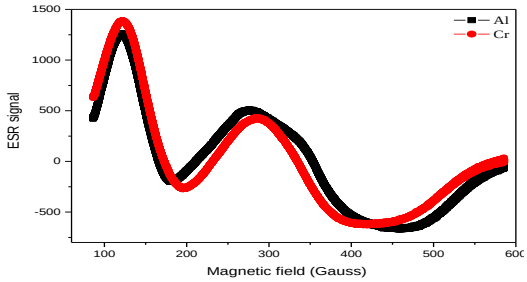

Fig. 9 ESR spectrum of $Ni_{0.7}Zn_{0.2}Cu_{0.1}Fe_{1.9}M_{0.1}O_4$ (M=Al and Cr)

3.9 Vibrating Sample Magnetometer (VSM)

Fig. 10 shows the recorded hysteresis loops for the $Ni_{0.7}Zn_{0.2}Cu_{0.1}Fe_{1.9}M_{0.1}O_4$ (M=Al and Cr) ferrites with a maximum applied field up to 15000 Oe. It is illustrated that the loops have a narrow hysteretic behaviour characteristic of the soft magnetic nature of the samples. It is observed that the saturation magnetization (M_s) and magnetic moment (M_r) increase on Al^{3+} substituted compound than Cr^{3+} compound but the coercivity (H_c) decreases. The increase in saturation magnetization in Al^{3+} substituted compound may be explained by the formation of some agglomerates which could also be evidenced from SEM micrograph and also may be due to the extensive degree of particle coarsening, which in turn decreases the surface defect with respect to the volume of the particle. The decrease in saturation magnetization in Cr^{3+} substituted compound could be due to either of two reasons. Primarily, it may be due to crossover from single domain to multi-domain phase with increasing size. Secondly, it may be due to combination of surface effect and its surface anisotropy. Also, the decrease in saturation magnetisation at small sizes is attributed to the effects of the relatively dead or inert surface layer that has low magnetisation. Because of this high degree of homogeneous single crystalline phase and also due to the absence of impurities, the observed variation in the saturation magnetization is attributed to the variation of particle size of the samples. Such type of behaviour is earlier reported for different ferrites. The decrease of coercivity (H_c) in Al^{3+} substituted compound influenced by many factors, such as grain size, shape, packing density and the crystal defects. In this case, the coercivity diminishing may be attributed to the grain size of the materials and corresponding domain rotation process [31, 32].

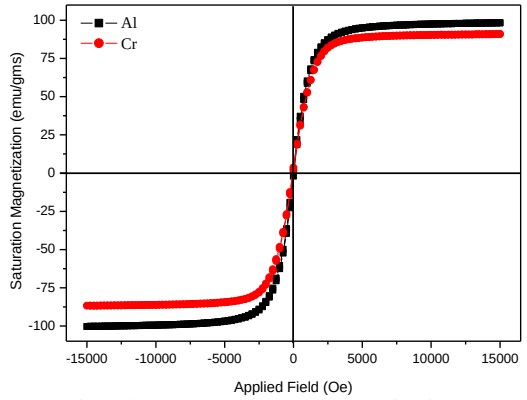

Fig. 10 Hysteresis loops for $Ni_{0.7}Zn_{0.2}Cu_{0.1}Fe_{1.9}M_{0.1}O_4$ (M=Al and Cr)

4. Conclusion

The ferrite system $Ni_{0.7}Zn_{0.2}Cu_{0.1}Fe_{1.9}M_{0.1}O_4$ (M=Al and Cr) ferrites are successfully synthesised by solid state reaction method using AR grade metal oxides. The X-ray diffraction results showed the formation of single phase cubic spinel structure. The crystallite size and lattice constant are in the reported range. The SEM analysis indicates the uniform grain growth and less agglomeration. The FTIR spectra for both the samples show the presence of two distinct transmittance bands with slight change in the band position. The DC resistivity of both the samples decreases with increase in frequency up to 100 MHz. The resonance field decreases whereas g-value increases in Cr^{3+} substituted ferrite system this is due to the isotropic alignment of magnetic moments with substituted ions. The saturation magnetization (M_s) and magnetic moment (M_r) are increase with Al^{3+} substituted ferrite system but the coercivity (H_c) decreases.

Acknowledgement

I gratefully acknowledge the funding agency, the Department of science and technology (DST) of the Government of India, for providing research support, to complete my thesis work, in the form of DST-PURSE.

References

[1] R.A. McCurie, Ferromagnetic materials, structure and properties, Academic Press, San Diego, 1994.
[2] Alex Goldman, Modem ferrite technology", 2nd Ed., Springer Science-Business Media, Inc., New York, 2006.
[3] F. Li, J.J. Liu, D.G. Evans, X. Duan, "Stoichiometric synthesis of pure MFe_2O_4 (M= Mg Co, and Ni) spinel ferrites from tailored layered double hydroxide (hydrotalcite-like) precursors, Chem. Mater. 16 (2004) 1597-1602.
[4] O.F. Caltum, L. Spinu, A.I. Stancu, L.D. Thung, W. Zhou, Study of the microstructure and of the permeability spectra of Ni-Zn-Cu ferrites, J. Magn. Magn. Mater. 242-245 (2002), 162-162.
[5] D.R. Patil, B.K. Chougule, Effect of copper substitution on electrical and magnetic properties of $NiFe_2O_4$ ferrite, Mater. Chem. Phys. 117 (2009) 35-40.
[6] P.B. Belavi, G.N. Chavan, L.R. Naik, R. Somashekar, R.K. Kotnala, Structural, electrical and magnetic properties of cadmium substituted nickel-copper ferrites, Mater. Chem. Phys. 132 (2012) 138-144.
[7] F.S. Li, L. Wang, J.B. Wang, Q.G. Zhou, X.Z. Zhou, H.P. Kunkel, G. Williams, Site preference of Fe in nanoparticles of $ZnFe_2O_4$, J. Magn. Magn. Mater. 268 (2004) 332-339.
[8] S. Al Morrison, C. Ll Cahill, E.E. Carpenter, S. Calvin, R. Swaminathan, M.E. McH enry, V.G. Harris, Magnetic and structural properties of nickel zinc ferrite nanoparticles synthesized at room temperature, J. Appl. Phys. 95 (2004) 6392-6395.
[9] B. Ghosh, M. Sardar, S. Banerjee, Effect of antisite formation on magnetic properties of nickel zinc ferrite particles, J. Appl. Phys. 114 (2013) 183903-183904.
[10] A.V. Raut, P.P. Khirade, A. Humbe, S.A. Jadhav, D.R. Shengule, Structural, electrical, dielectric and magnetic properties of Al^{3+} substituted Ni-Zn ferrite, J. Supercond. Novel Magn. 29 (2016) 1331-1337,
[11] M.B. Hossen, A.K.M.A. Hossain, Influence of Al^{3+} substitution on impedance spectroscopy studies of $Ni_{0.27}Cu_{0.10}Zn_{0.63}Al_xFe_{2-x}O_4$, Adv. Mater. Lett. 6(9) (2015) 810-815.
[12] K.R. Rahman, F.U.Z. Choudhury, M.N.I. Khan, Structural, morphological and magnetic properties of Al^{3+} substituted $Ni_{0.25}Cu_{0.20}Zn_{0.55}Al_xFe_{2-x}O_4$ ferrites synthesized by solid state reaction route, Result Phys. 7 (2017) 354-360.
[13] M.K. Fayek, S.S. Ata Allah, Fe Mössbauer and electrical studies of the (NiO)-$(Cr_2O_3)_x$-$(Fe_2O_3)_{2-x}$ system, Phys. Status Solid. A 198 (2003) 457-464.
[14] A.M. Gismelseed, A.A. Yousif, Mössbauer study of chromium-substituted nickel ferrites, Phys. B 370 (2005) 215-222.
[15] Seema Sharma, Kavita Verma, Umesh Chaubey, Vidyanand Singh, B.R. Mehta, Influence of Zn substitution on structural, microstructural and dielectric properties of nanocrystalline nickel ferrites, Mater. Sci. Eng. B 167 (2010) 187-192.
[16] Le-Zhong Li, Xiao-Xi Zhong, Rui Wang, Xiao-Qiang Tu, Structural, magnetic and electrical properties of Zr-substitued NiZnCo ferrite nanopowders, J. Magn. Magn. Mater. 435 (2017) 58-63.
[17] V.D. Sudheesh, J. Nehra, A. Vinesh, V. Sebastian, N. Lakshmi, D.P. Dutta, et al., Investigation of structural and magnetic properties of $Ni_{0.5}Zn_{0.5}Fe_2O_4$ nano powders prepared by self-combustion method, Mater. Res. Bull. 48 (2013) 698-704.
[18] M.Y. Lodhi, K. Mahmood, A. Mahmood, H. Malik, M.F. Warsi, I. Shakir, M. Asghar, M.A. Khan, New $Mg_{0.5}Co_xZn_{0.5-x}Fe_2O_4$ nano-ferrites: structural elucidation and electromagnetic behavior evaluation, Curr. Appl. Phys. 14 (2014) 716-720.
[19] A. Maqsood, K. Khan, M. Anis-ur-Rehman, M.A. Malik, Spectroscopic and magnetic investigation of NiCo nanoferrites, J. Alloys Compd. 509 (2011) 7493-7497.
[20] N. Rezlescu, E. Rezlescu, C. Pasnicu, M.L. Craus, Effects of the rare-earth ions on some properties of a nickel-zinc ferrite, J. Phys.: Condens. Matter 6 (1994) 5707-5716.
[21] K. Vijaya Babu, G.V. Santosh Kumar, K. Jalaiah, P.T. Shibeshi, Effects of copper substitution on the microstructural, electrical and magnetic properties of $Ni_{0.7}Co_{0.3-x}Cu_xFe_2O_4$ ferrites, J. Phys. Chem. Solids 118 (2018) 172-185.
[22] S.E. Shirsath, B.G. Toksha, K.M. Jadhav, Structural and magnetic properties of In3þ substituted $NiFe_2O_4$, Mater. Chem. Phys. 117 (2009) 163-168.
[23] T. Ramesh, R.S. Shinde, S.R. Murthy, Synthesis and characterization of nanocrystalline $Ni_{0.94}Co_{0.03}Mn_{0.04}Cu_{0.03}Fe_{1.96x}Al_xO_4$ ferrites for microwave device applications, J. Magn. Magn. Mater. 345 (2013) 276-281.
[24] M. Kaiser, Magnetic and dielectric properties of low vanadium doped nickel-zinc-copper ferrites, J. Phys. Chem. Solids 71 (2010) 1451-1457.

https://doi.org/10.30799/jnst.157.18040507

Cite this Article as: G. Satyanarayana, G. Nageswara Rao, K. Vijaya Babu, Structural, dielectric and magnetic properties of Al^{3+} and Cr^{3+} substituted Ni-Zn-Cu ferrites, J. Nanosci. Tech. 4(5) (2018) 487–491.

[25] K. Jalaiah, K. Vijaya Babu, K. Chandra Mouli, P.S.V. Subba Rao, Effect on the Structural, DC resistivity and magnetic properties of Zr and Cu co-substituted $Ni_{0.5}Zn_{0.5}Fe_2O_4$ using sol-gel auto-combustion method, Phys. B: Condens. Matter 534 (2018) 125-133.
[26] K. Jalaiah, K. Vijaya Babu, Structural, magnetic and electrical properties of nickel doped Mn-Zn spinel ferrite synthesized by sol-gel method, Journal of Magnetism and Magnetic Materials, 423, 275-280, 2017.
[27] J.S. Ghodake, T.J. Shinde, R.P. Patil, S.B. Patil, S.S. Suryavanshi, Initial permeability of Zn-Ni-Co ferrite, J. Magn. Magn. Mater. 378 (2015) 436-439.
[28] Gagan Kumar, Jagdish Chand, Satish Verma, M. Singh, Mixed Mg-Mn ferrites for high frequency applications processed by citrate precursor technique, J. Phys. D: Appl. Phys. 42 (2009) 155001-155006.
[29] M. Deepty, Ch. Srinivas, K. Vijaya Babu, E. Ranjit Kumar, S.S. Meena, et al., Structural and electron spin resonance spectroscopic studies of $Mn_xZn_{1-x}Fe_2O_4$ (x=0.5, 0.6, 0.7) nano-ferrites synthesized by sol-gel auto-combustion method, J. Magn. Magn. Mater. 466 (2018) 60-68.
[30] S.A.V. Prasad, P.N. Ramesh, M. Deepty, G. Prasad, K. Srinivasa Rao, et al., Synthesis of MFe_2O_4 ($M=Mg^{2+}$, Zn^{2+}, Mn^{2+}) spinel ferrites and their structural, elastic and ferromagnetic resonance properties", Ceram. Int. 44 (2018) 10517-10524.
[31] A.V. Knyazev, I. Zakharchuk, E. Lähderanta, K.V. Baidakov, S.S. Knyazeva, I.V. Ladenkov, Structural and magnetic properties of Ni-Zn and Ni-Zn-Co ferrites, J. Magn. Magn. Mater. 435 (2017) 9-14.
[32] H.E. Zhang, B.F. Zhang, G.F. Wang, X.H. Dong, Y. Gao, The structure and magnetic properties of $Zn_{1-x}Ni_xFe_2O_4$ ferrite nanoparticles prepared by sol-gel auto-combustionJ. Magn. Magn. Mater. 312 (2007) 126-130.

https://doi.org/10.30799/jnst.157.18040507

Cite this Article as: G. Satyanarayana, G. Nageswara Rao, K. Vijaya Babu, Structural, dielectric and magnetic properties of Al^{3+} and Cr^{3+} substituted Ni-Zn-Cu ferrites, J. Nanosci. Tech. 4(5) (2018) 487–491.